Composite Structures 290 (2022) 115522

Contents lists available at ScienceDirect

Composite Structures

journal homepage: www.elsevier.com/locate/compstruct

An extrapolation method to remove spurious stress concentration in micromechanical analyses of composites using pixel-based meshes

Hemanth Thandaga Nagaraju, Bhavani V. Sankar *, Nam-Ho Kim, Ghatu Subhash

Department of Mechanical and Aerospace Engineering, University of Florida, Gainesville, FL, USA

ARTICLE INFO

Keywords:
Micromechanics
Finite element analysis (FEA)
Voxel meshes
Artificial stress concentration

ABSTRACT

It is easier to generate a finite element mesh of complicated geometries with voxel-based meshes compared to conformal meshes. However, the local stresses in voxel-based meshes are higher owing to artificial stress concentration caused due to jagged lines that approximate a curve. We propose a method that accounts for this anomaly which would lead to accurate prediction of maximum von Mises stress in voxel-based meshes. The method is based on the variation of reciprocal of stresses and associated numerical gradient. The prediction of the proposed method is compared against the results of a conformal mesh by considering four two-dimensional example problems. The accuracy of the proposed method is verified using different mesh densities, material properties, and integration schemes. The proposed method was also implemented on a conformal mesh to verify that it filters out just the spurious stress concentration and not the realistic stress concentration.

1. Introduction

Finite element (FE) based micromechanics has been widely used in the study of textile composites to calculate the effective elastic constants [1–3]. The linear elastic analysis often involves the identification of the smallest building block of the textile composite called a repeatable unit cell (RUC) followed by the imposition of periodic boundary conditions on the FE mesh of the RUC [4–8]. The process of obtaining an FE mesh of RUC of textile composite is not a straightforward process due to the presence of undulating, interweaving yarns and associated complicated textile architecture. Furthermore, the generated FE mesh needs to be homologous to apply periodic boundary conditions [9]. These requirements are relatively easy to satisfy in the voxel meshing technique. The computational advantages of using a voxel mesh over other meshes such as structured mesh, grid-based mesh, and unstructured triangular meshes can be found in the works of Kim et al. [10]. The voxel meshes can be generated through preprocessing modeling software such as TexGen^{TM} [11,12]. In voxel mesh, the domain of interest is discretized into an almost uniform rectangular arrangement of hexahedrons. These hexahedron elements are assigned values of material properties based on the yarn volume fraction calculated for an individual element which eventually depends on the location of the centroid of each element. This means that each finite element is either assigned a yarn or a matrix property. Therefore, the boundary separating the yarn and the matrix in voxel mesh is facetted, stepped jagged, or zigzag rather than a smooth curve. This staircase-like boundary produces artificially high stresses in its vicinity [13–15]. The material discontinuity at the boundary is a legitimate reason for stress concentration. However, the zigzag boundary exaggerates the stress concentration which is not present in the actual material. This anomaly is a local phenomenon that does not show up when the local stresses are averaged over the domain to obtain macro-stresses. Hence, many works can be found in the literature that have used voxel meshes to calculate the homogenized elastic constants of textile composites [10,11,16,17]. However, it might not be accurate to predict the failure of the composite based on the local maximum stresses due to artificial stress concentration. It is also known from the literature that even though increasing the mesh density leads to a better approximation of yarn geometry, it does not resolve the aforementioned mesh artifact. TexGen^{TM} does have the capability to produce conformal meshes with tetrahedron elements but such meshes are susceptible to element distortions, low element volumes if the mesh is not properly seeded, and in general, require a greater number of elements than hexahedron mesh. The quality of tetrahedron mesh is further worsened if it is used to generate FE mesh of curved RUC for the analysis of textile composite tubes [18]. Thus, even though it is computationally favorable to use voxel-based meshes, their use is limited to the prediction of effective elastic constants of textile composites. The micromechanical models that are based on local stresses like direct micromechanics [19]

* Corresponding author.
E-mail address: sankar@ufl.edu (B.V. Sankar).

https://doi.org/10.1016/j.compstruct.2022.115522
Received 9 December 2021; Received in revised form 18 March 2022; Accepted 21 March 2022
Available online 24 March 2022

cannot be used in analyses that use voxel meshes.

There are few works that address this limitation. Fang et al. used a weighted averaging technique to alleviate the spurious high stresses in voxel meshes [13]. In this method, the stresses in layers of elements, in the neighborhood of the zigzag boundary were averaged. The averaged layers of elements had the same material properties. Fang et al. illustrated this method by considering different numbers of layers in the vicinity of the zigzag boundary. They also tried different weighted averaging schemes by considering different weight functions. However, all the averaging schemes gave relatively similar results and it is unclear if their preferred method of the two-layer averaging scheme [20] would work in other applications. A different averaging scheme is also found in the literature [14]. However, in these averaging schemes, there is no quantitative way of deciding the domain over which local stresses are to be averaged. There have been other pre-processing methods to approximate the zigzag boundary through a smoother curve by appropriate movement of nodes [21]. However, moving nodes of a yarn element implies that the material coordinate system must be redefined for every yarn element which complicates the mesh generation process.

Thus, it would be helpful if there was a method to account for spurious stress in the voxel-based mesh. Working in that direction, we propose a novel method to minimize artificial stress concentration observed in voxel meshes. This method is a post-processing procedure that will not affect the computation in FE solvers. The proposed procedure is compared against the results of conformal mesh (where the boundary is smooth) by considering von Mises stress. The two-dimensional problems were intentionally chosen so that both pixel-based (which is a two-dimensional analog of voxel-based mesh) and conformal meshes can be easily generated. The robustness of the proposed method was evaluated by considering two examples of material discontinuity and two example problems of plates with a hole. The plates with a hole example problems were considered as the maximum stress can be calculated by using the stress concentration factors. The emphasis was on developing a method to filter out the artificial stress concentration rather than dealing with a complicated problem. The proposed procedure called the *extrapolation method* can be easily adapted to three-dimensional meshes.

2. Methodology

We intend to estimate the maximum von Mises stress from pixel-based mesh which is closer to the maximum von Mises stress observed in the conformal mesh. The following examples are considered:

1) Unidirectional composite under transverse tension,
2) Unidirectional composite under shear strain,
3) Finite width plate with a circular hole subjected to uniaxial tension, and
4) Finite width plate with an elliptical hole subjected to uniaxial tension.

A linear elastic response was assumed in all four cases.

2.1. Generation of pixel-based meshes

To generate pixel-based mesh, the domain of interest is discretized uniformly to form an array of rectangles. For problems involving material discontinuity, an element is assigned a material property of either fiber or matrix depending on its nodal coordinates. For instance, an element is assigned a fiber property only if all its nodes are within the fiber, otherwise, a matrix property is assigned to it. A 2-D RUC of the unidirectional composite was modeled by both pixel-based mesh and conformal mesh. A quarter model of RUC (shown in Fig. 1) was employed to analyze unidirectional composite under uniaxial transverse tension while a full model was used to analyze unidirectional composite under shear strain. In the problems involving geometric discontinuity such as a hole, a similar idea was adapted wherein the nodes that lie within the radius of the hole were deleted, resulting in a pixel-based mesh. The conformal meshes were generated using the pre-processing modeling features available in ABAQUS 2019 software.

2.2. The pre-processing steps

The quarter model and the boundary conditions for the unidirectional composite under uniaxial tension are shown in Fig. 1. The specified displacements were $u_x = 0$ alongAB, $u_y = 0$ along AD, $u_y = 2mm$ alongBC, and CD was traction free where u_i refers to the displacement in i direction.

In the case of the unidirectional composite under shear load, periodic boundary conditions were imposed on the full model of RUC:

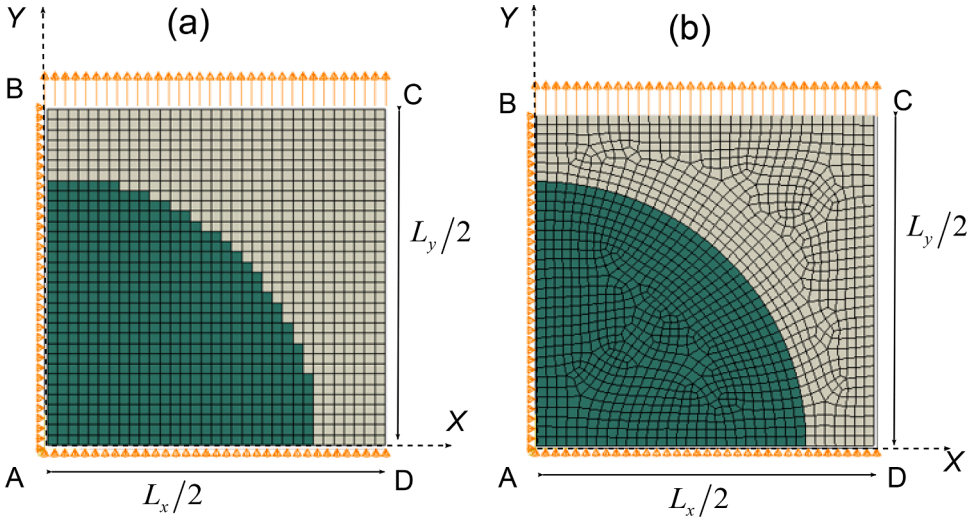

Fig. 1. The quarter model of RUC was used to analyze unidirectional composite under transverse tension. The pixel-based mesh (a) has a zigzag path separating the fiber–matrix boundary while the conformal mesh (b) has a smooth fiber–matrix boundary. The fiber elements are in green and the matrix elements are in grey. (For interpretation of the references to colour in this figure legend, the reader is referred to the web version of this article.)

$$\begin{aligned} u_x(L_x/2,y) - u_x(-L_x/2,y) &= 0 \\ u_y(L_x/2,y) - u_y(-L_x/2,y) &= \frac{\gamma_{xy}}{2}L_x \\ u_x(x,L_y/2) - u_x(x,-L_y/2) &= \frac{\gamma_{xy}}{2}L_y \\ u_y(x,L_y/2) - u_y(x,-L_y/2) &= 0 \end{aligned} \tag{1}$$

where γ_{xy} is non-zero shear strain, L_x and L_y are dimensions of the RUC as shown in Fig. 1.

For problems of finite width plates with a hole, remote traction of 50 MPa was applied in the x-direction and a quarter model as shown in Figs. 2 and 3 was used.

The proposed procedure was implemented for different meshes (namely coarse and finer), different integration schemes (namely reduced and full integration schemes), and different materials (namely M1, M2, and M3). This not only helped us in assessing the robustness of the proposed method but also in understanding how artificial stress concentration affects the maximum von Mises stress in different meshes. The number of elements in coarse and fine mesh for each pixel-based and conformal mesh is presented in Table 1. It can be observed that the number of elements in the conformal and pixel-based mesh is comparable for unidirectional composite problems. However, for the plate problems, there is a significant difference between the number of elements in the two meshes. This is due to the presence of a hole in the conformal mesh, which meant that the mesh had to be refined near the geometric discontinuity. Furthermore, the mesh size of pixel-based mesh was required to be decreased so that the maximum stress in pixel-based mesh exceeded stress from empirical solutions and facilitate a valid comparison between the results of conformal and pixel-based meshes.

2.3. The extrapolation method:

The minimum and maximum von Mises stresses in the vicinity of a discontinuity in the pixel-based mesh are exaggerated due to the zigzag boundary of discontinuity such as a hole or an inclusion. We intend to filter out this factitious effect and accurately predict the maximum von Mises stress from the results of pixel-based mesh. The *extrapolation method*, which was used for this purpose is explained in the rest of this section by considering the FE-generated von Mises stresses in fiber elements of the unidirectional composite under transverse tension. However, the extrapolation method can be used to remove artificial stress concentration in other stresses as well.

The first step involves extracting the von Mises stresses at the integration points (or at nodes). This is followed by calculating the reciprocal of von Mises stresses and sorting the reciprocal values in ascending order as shown in Fig. 4. The least reciprocal value corresponds to the maximum value of von Mises stress. We intend to estimate the accurate value of maximum von Mises stress by considering their reciprocals. Thus, in this study, we are interested in the accurate prediction of the least reciprocal value of von Mises stress. In Fig. 4, the horizontal axis represents the rank of the reciprocal value. The least reciprocal value is ranked 1, while the highest rank is equal to about 70% of the data points. Although the data points beyond 70% have lower stress values, they could have significant gradients (i.e. stress values could drop drastically) and possibly affect the results. To circumvent such confounding effects, the last 30% of data points were not considered in further analysis. It can be observed that the curve in Fig. 4 is almost vertical initially and then it starts flattening out. The sudden change in slope at point B is of interest. The reciprocal values in the regionAB correspond to spurious von Mises stresses that are produced in the fiber as an artifact of pixel-based mesh discretization and may not be realistic. To resolve this mesh artifact, we consider 30 data points ahead of point B (i.e., region BC) as the trustworthy region for reasons explained in the rest of this section. It should be mentioned that the choice of 30 data points is arbitrary but is based on our experience with many analyses. The region BC represents the true stress values that are based on the physics of the problem rather than the mesh artifact. A linear equation is fit to the trustworthy region BC such that reciprocal value is the dependent variable and rank is the independent variable. The inverse of the intercept (point A' in Fig. 4) of the fit equation is then considered as the real value of the maximum von Mises stress.

It can be observed that successful identification of the trustworthy region is key to accurate prediction of maximum von Mises stress. Thus, a mathematical procedure involving the numerical gradient of the curve shown in Fig. 4 was used to objectively identify the point$B$. The numerical gradient was calculated by using MATLAB built-in function *gradient* that calculates the gradient of $n-$dimensional vector a based on the central difference method [22]:

$$G = gradient(a) = \left\{ \begin{array}{c} G(1) = a(2) - a(1) \\ G(i) = 0.5(a(i+1) - a(i-1)), \forall i = 2,3,...,n-1 \\ G(n) = a(n) - a(n-1) \end{array} \right\} \tag{2}$$

As the gradient was noisy, it was smoothed twice by using MATLAB built-in function *smooth* based on Savitzky-Golay filter with a span of five and polynomial of degree one [23]. The relatively high values of smoothed gradients were identified by considering their z-score which was calculated as:

$$z - score = \frac{(smoothed\_gradient) - mean(smoothed\_gradients)}{std(smoothed\_gradients)} \tag{3}$$

where $std(smoothed\_gradients)$ is the standard deviation of the smoothed gradients.

The z-score measures how far a value is from the mean of the data in terms of the standard deviation. The z-score of smoothed gradients was as shown in Fig. 5, where the start of the trust-worthy region corresponds to the rank when the z-score drops to zero for the first time. It is represented by point$B$. The 30 data points from B form the required trustworthy region as shown in Fig. 5. This method of choosing the trustworthy region by considering $z\text{-}score = 0$ gave reasonably accurate results for the problems of unidirectional composites. The premise here

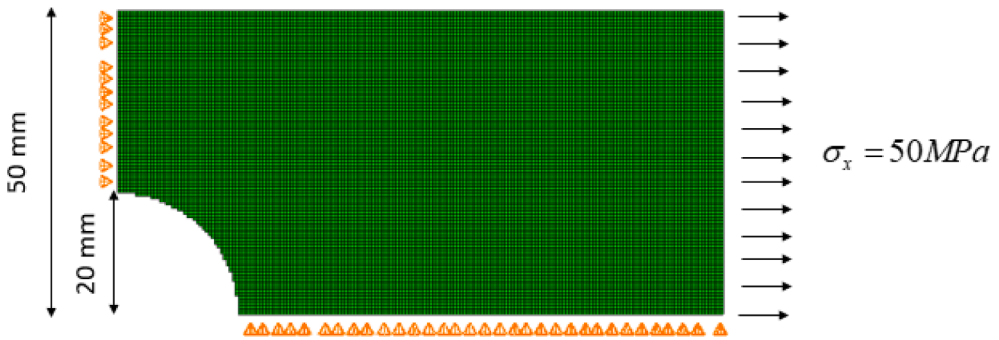

Fig. 2. The dimensions and boundary conditions of the FE model for a finite plate with a circular hole.

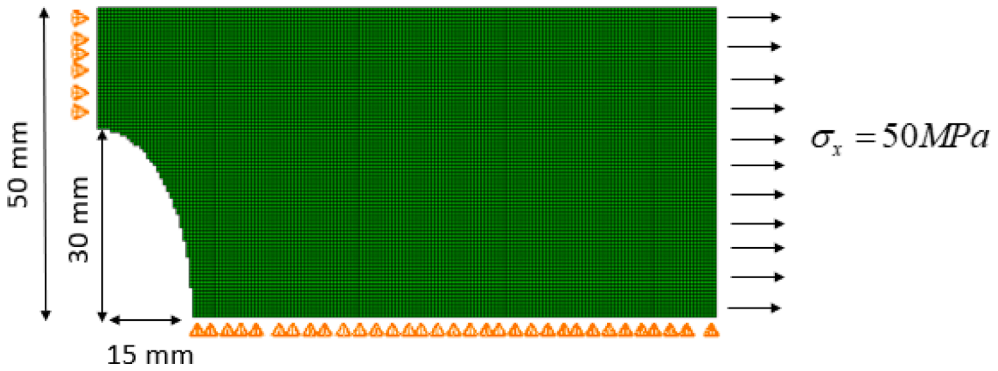

Fig. 3. The dimensions and boundary conditions of the FE model for a finite plate with an elliptical hole.

Table 1
The number of elements in each of the meshes considered in this study.

Mesh type	Unidirectional composite				Finite width plate			
	Transverse tension		Shear strain		Circular hole		Elliptical hole	
	Pixel-based	Conformal	Pixel-based	Conformal	Pixel-based	Conformal	Pixel-based	Conformal
Coarse mesh	1,369	1,337	8,464	8,333	18,744	120,434	51,609	17,057
Fine mesh	12,321	12,311	17,689	18,740	38,275	22,540	116,059	52,182

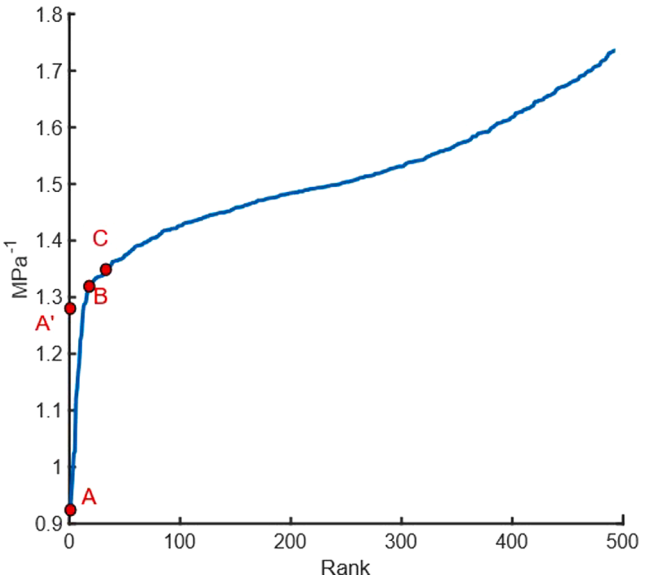

Fig. 4. The reciprocal of von Mises stresses produced in fiber elements when the unidirectional composite is under transverse tension.

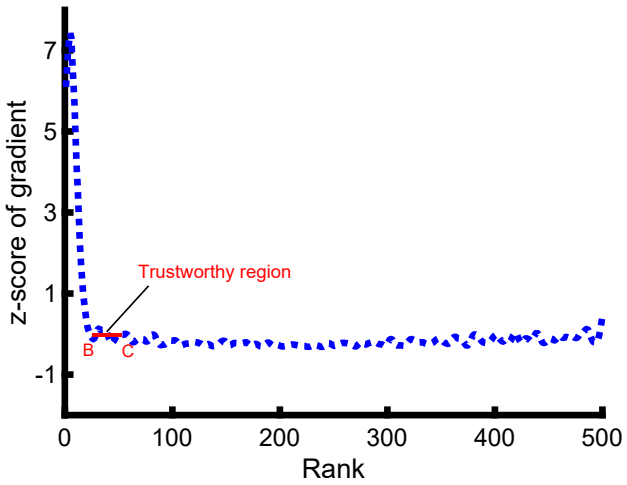

Fig. 5. The z-score of smoothed gradients. The point B is identified when the z-score equals 0 for the first time and 30 data points from there on is the trustworthy region.

was that the realistic stress value cannot increase abruptly but rather approach the maximum value smoothly without drastic changes in the slope along its ascent. However, this does not hold for a finite width plate with geometric discontinuity such as a circular hole or an elliptical hole as the stresses increase rapidly at the vicinity of the hole. Hence, choosing *z-score = 0* might remove the realistic stress concentration for plates of finite width and a hole. The discussed procedure was repeated at different values of *z-score* and it was found that *z-score = 8* gave reasonable results which are further discussed in the next section. The key steps in this procedure are summarized as follows:

1) Extract the von Mises stresses.
2) Calculate the reciprocal of von Mises stresses and sort them in ascending order. In subsequent steps consider the first 70% of reciprocal values.
3) Calculate the numerical gradient of sorted reciprocals and smoothen them based on the Savitzky-Golay method (with a span of 5 and polynomial of degree 1). This smoothening operation is done twice to reduce excessive fluctuations.
4) Calculate the z-score of the smoothened gradients. At *z-score = 0* (point *B*) and 30 data points beyond that (towards right in Fig. 5) form the trustworthy region, and finally
5) Fit a linear equation to the trustworthy region and consider the reciprocal of the equation's intercept as the maximum value.

In this study, the extrapolated value represents the reciprocal of realistic maximum von Mises stress. Indeed, the maximum von Mises stress predicted by the pixel/voxel mesh at the zigzag boundary is inaccurate. However, the von Mises stress values at the finite elements sufficiently far away from the zigzag boundary are less influenced by the discretized modeling approach. The success of pixel/voxel-based mesh in predicting the effective elastic constants is proof that the stress values

at a sufficient distance from the zigzag boundary are useful. But, if the extrapolation is based on values very far away from the zigzag boundary, then the extrapolated value might not be a true representation of the reciprocal von Mises stress. The z-score of the numerical gradient ensures that the trustworthy region is at an optimal distance from the zigzag boundary and makes the reciprocal stresses of the trustworthy region reliable enough.

As stated in the introduction, the emphasis was on simpler 2-D problems where the analytical solution was readily available (plates of finite width with a hole) or where the generation of either conformal mesh or pixelized mesh did not pose a challenge. This choice was intentional to focus on developing a method to filter out the artificial stress concentration in the pixelized mesh.

3. Results and discussions

In this study, the results of conformal mesh were treated as the benchmark solution. The performance of the pixel-based mesh, *extrapolation method*, and the averaging scheme proposed by Fang et al. [13] were evaluated by comparing the respective results with that of the conformal model.

3.1. Unidirectional composite under transverse tension

The analysis was carried out for different materials and different integration schemes. The material properties are given in Table 2. The corresponding results of maximum von Mises stresses are shown in Table 3. The reported percentage of error is relative to the results of conformal mesh. The contour plot of von Mises stresses is shown in Fig. 6, from which it can be inferred that those elements closer to the zigzag (step-like) boundary show high spurious stresses. These spurious stresses do not vanish away even for finer meshes, which is consistent with the observations made in the previous studies [13,24]. It is noted that the distribution of von Mises stresses in the conformal mesh is different from that of a pixel-based mesh. However, this study is only concerned with the prediction of maximum von Mises stress from pixel-based mesh after considering the artificial stress concentration.

It is seen from the similar maximum von Mises stresses in conformal meshes with M2 material, that the solution had converged at coarse mesh itself. It can be observed from Table 3 that the proposed *extrapolation method* performs better than the averaging method proposed by Fang et al. [13]. The results further show that the full integration scheme is most detrimental in pixel-based meshes as it exaggerates the highest von Mises stress by more than 100%. For the identical mesh and integration scheme, the relative error of pixel-based mesh is highest at 87% for M3 (for which Young's modulus of fiber is 40 times that of the matrix) and is least at 15% for M1 (for which Young's modulus of fiber is 2.5 times that of the matrix). Thus, it can be noted from Tables 2 and 3, that exaggeration of highest von Mises stress is a function of the difference in elastic constants of fiber and matrix. Therefore, in a particular material system, if the fiber and matrix properties are comparable to each other, then local stress-based analysis through pixel-based meshes might be an innocuous approach. However, the error in pixel-based mesh drops to within 16% across the considered cases when the *extrapolation method* is implemented. It can also be observed that when the *extrapolation method* is implemented on a conformal mesh, the prediction error is less than 2% across material systems, mesh densities, and integration schemes considered in this study which means that the *extrapolation method* preserves much of the realistic stress concentration.

Table 2
The material properties used in this study.

Material	Young's modulus (MPa)		Poisson's ratio	
	Fiber	Matrix	Fiber	Matrix
M1	2.5	1	0.35	0.3
M2	10	1	0.35	0.3
M3	40	1	0.35	0.3

3.2. Unidirectional composite under shear load

The contour plot of von Mises stress for unidirectional composite under in-plane shear is shown in Fig. 7. It can be observed that the values of von Mises stress in the first quadrant are repeated in the other three quadrants. Thus, to avoid duplicity only the values of fiber elements in the first quadrant were considered in the *extrapolation method* detailed earlier in Section 2.3. The stresses in fiber elements in the pixel-based mesh were higher than those observed in the conformal mesh. The results are summarized in Table 4. The error in pixel-based meshes is higher for full integration and M3 material. These results are consistent with results observed in unidirectional composite under transverse tension discussed in Section 3.1. The *extrapolation method* consistently yields results that are closer to that of conformal mesh. The performance of the *extrapolation method* and the averaging scheme proposed by Fang et al. [13] are as shown in Table 4. It is seen that when the extrapolation method is implemented on the results of a conformal mesh, the prediction error is within 2%, thus preserving the realistic stress concentration which was also observed in Section 3.1.

In the following section, we shall adopt the *extrapolation method* to remove stress concentration in problems having geometric discontinuities.

3.3. Analysis of a finite width plate with a circular hole

In this example, a homogeneous plate of finite width with a circular hole, shown in Fig. 2, is subjected to uniaxial tension. Unlike the previous unidirectional composite examples, the stress concentration due to the presence of a hole can be calculated by appropriate stress concentration factors. The plate was assumed to be homogeneous and of unit thickness. The stress concentration factor based on the dimensions shown in Fig. 2 was found to be 2.24 relative to nominal stress [25]. The maximum von Mises stresses are shown in Table 5. The FE analysis was carried out by considering a quarter model as shown in Fig. 2. The maximum values of σ_{xx} in a conformal mesh were 186 MPa, 189 MPa, 186 MPa in coarse mesh with reduced integration, coarse mesh with full integration, and fine mesh with reduced integration, respectively, which is consistent with the expected maximum stress of 187 MPa based on the empirical stress concentration factors [25].

The maximum von Mises stress in the pixel-based mesh is more than 30% of the von Mises stress predicted in conformal mesh due to the spurious stress concentration. It was earlier stated that the *z-score = 0* criterion will not identify the start of the trustworthy region in the case of plates of finite width with a hole. Therefore, to find an appropriate criterion, the extrapolation technique was carried out at different values of z-score ranging from 0 to 10 in increments of 1. The error from each z-score was calculated for both conformal and pixel-based meshes and were as shown in Figs. 8 and 9. It can be observed that the error in the conformal mesh is almost insensitive to the z-score. This means that the slope of the reciprocal von Mises stress does not change drastically in the conformal mesh. However, in pixel-based mesh, it can be observed that the error changes from −35% to 2% for a plate with a circular hole as shown in Fig. 8. The error for a plate with an elliptical hole changes from −45% to −5% as shown in Fig. 9. This proves that the slope of the reciprocal of von Mises changes drastically in pixel-based mesh due to the presence of sharp corners. From Figs. 8 and 9, *z-score = 8* was chosen as the criterion for identifying the start of the trustworthy region in the pixel-based mesh. Based on this criterion, the *extrapolation method* on pixel-based mesh predicted maximum von Mises stress to within 6% of the conformal mesh (see Table 5). It can also be seen that the realistic stress concentration in the conformal mesh is preserved when the *extrapolation method* is used on the conformal mesh. Additionally, the *extrapolation method* gives more accurate results than the smoothing

Table 3
The maximum von Mises stresses developed in the quarter model of RUC of the unidirectional composite under uniaxial transverse tension. The deviation relative to maximum von Mises stress calculated from conformal mesh is shown in parenthesis.

Material	Mesh	Conformal mesh (MPa)	Extrapolation method on conformal mesh (MPa)	Pixel-based mesh (MPa)	Extrapolation method on pixel-based mesh (MPa)	Smoothing method of Fang et al. on pixel-based mesh (MPa)
M1	Coarse mesh and reduced integration	0.3984	0.3941 (-1.08%)	0.4563 (15%)	0.4060 (2%)	0.4082 (2%)
M2	Coarse mesh and reduced integration	0.7227	0.7169 (-0.8%)	1.0819 (50%)	0.7744 (7%)	0.8028 (11%)
M2	Coarse mesh and full integration	0.7240	0.7224 (-0.22%)	1.7047 (135%)	0.8416 (16%)	0.8379 (16%)
M2	Finer mesh and reduced integration	0.7238	0.7213 (-0.35%)	1.0935 (51%)	0.7637 (6%)	0.7690 (6%)
M3	Coarse mesh and reduced integration	0.8943	0.8897 (-0.51%)	1.6708 (87%)	0.9844 (10%)	1.6052 (19%)

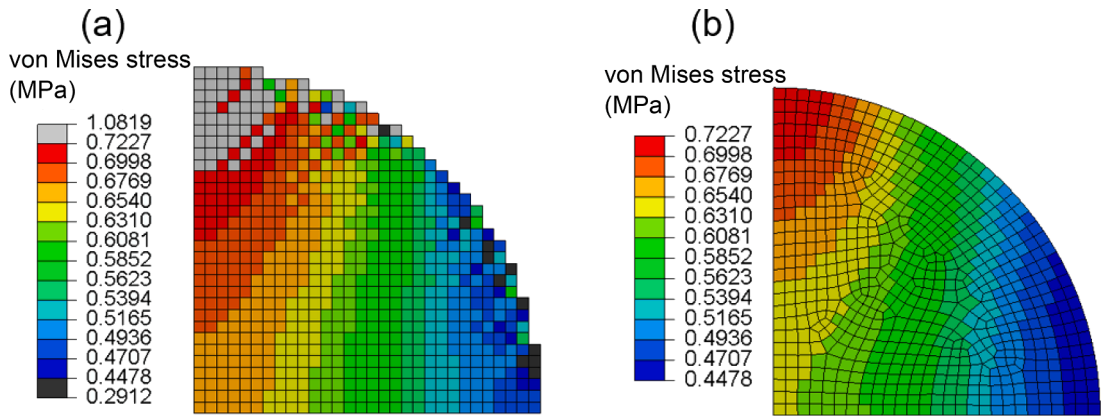

Fig. 6. The contour plot of von Mises stress in fiber elements in pixel-based mesh (a) and conformal mesh (b) when the unidirectional composite is under transverse tension.

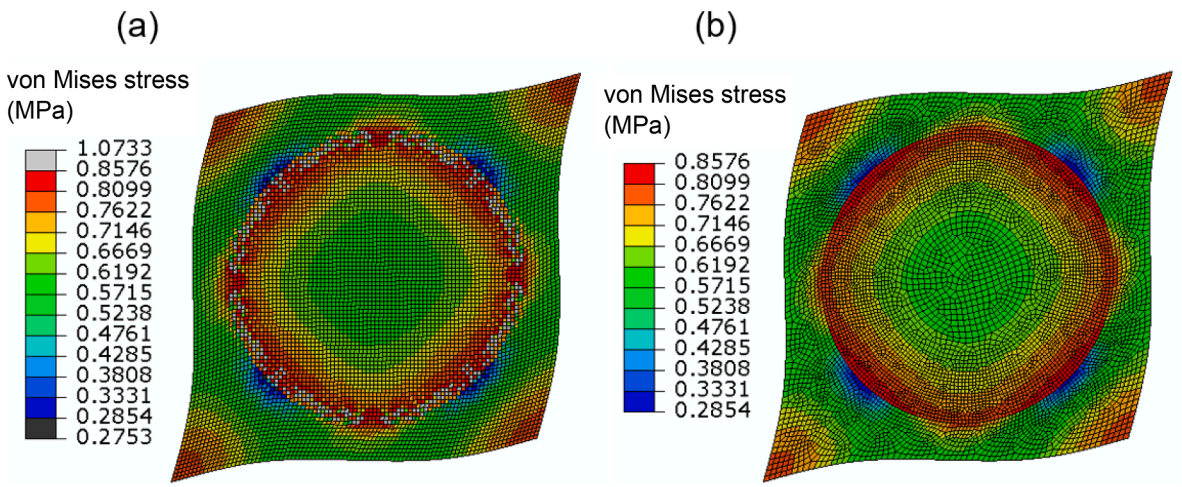

Fig. 7. The contour plot of von Mises stress in pixel-based (a) and conformal (b) mesh for a unidirectional composite under in-plane shear.

method proposed by Fang et al. [13].

3.4. Analysis of plate of finite width with an elliptical hole

The dimension of the plate and elliptical hole were given earlier in Fig. 3. The stress concentration factor based on the dimensions of the geometry was found to be 3 relative to nominal stress [25]. The maximum σ_{xx} were 379 MPa, 380 MPa, 376 MPa in coarse mesh with reduced integration, coarse mesh with full integration, and fine mesh with reduced integration respectively, in conformal meshes which is consistent with the expected maximum stress of 375 MPa based on empirical stress concentration factors [25]. From Table 6, it can be observed that the extrapolation method on pixel-based mesh predicts the highest von Mises stress to within 13% of the conformal mesh. As observed in Section 3.1, when the *extrapolation method* is implemented in a conformal mesh, the results are almost identical to the original values of the conformal mesh before applying the *extrapolation method*.

It is to be noted that the *extrapolation method*, predicts only the value of maximum von Mises stress and, it does not give any information on the location of predicted maximum von Mises stress. It also does not provide information on the altered stress distribution due to this artificially enhanced stress concentration. The method only helps remove the

Table 4
The observed results of maximum von Mises stress in fiber elements when the unidirectional composite is under shear load. The values in parenthesis are the deviations calculated relative to maximum von Mises stress from conformal mesh.

Material	Mesh	Conformal mesh (MPa)	Extrapolation method on conformal mesh (MPa)	Pixel-based mesh (MPa)	Extrapolation method on pixel-based mesh (MPa)	Smoothing method of Fang et al. on pixel-based mesh (MPa)
M1	Coarse mesh and reduced integration	0.5814	0.5815 (0.02%)	0.6047 (4%)	0.5998 (3%)	0.5843 (0.5%)
M2	Coarse mesh and reduced integration	0.8563	0.8568 (0.06%)	1.0733 (25%)	0.9957 (16%)	0.8657 (1%)
M2	Coarse mesh and full integration	0.8601	0.8510 (-1.06%)	1.574 (83%)	1.2059 (40%)	0.9046 (5%)
M2	finer mesh and reduced integration	0.8578	0.8569 (-0.10%)	1.1174 (30%)	0.9551 (11%)	0.8727 (2%)
M3	Coarse mesh and reduced integration	0.9723	0.9731 (0.08%)	1.6054 (65%)	1.2637 (30%)	1.1372 (17%)

Table 5
The comparison of maximum von Mises stress developed in a plate with a circular hole in the pixel-based mesh and conformal mesh. The values in parenthesis are the deviations calculated relative to maximum von Mises stress from conformal mesh.

Mesh	Conformal mesh (MPa)	Extrapolation method on conformal mesh (MPa)	Pixel-based mesh (MPa)	Extrapolation method on pixel-based mesh (MPa)	Averaging scheme of Fang et al. on pixel-based mesh (MPa)
Coarse mesh and reduced integration	186	186 (0.02%)	204 (10%)	181 (-3%)	159 (-14%)
Coarse mesh and full integration	187	187 (0.07%)	248 (33%)	176 (-6%)	157 (-16%)
Finer mesh and reduced integration	186	186 (0.21%)	213 (15%)	190 (2%)	168 (-10%)

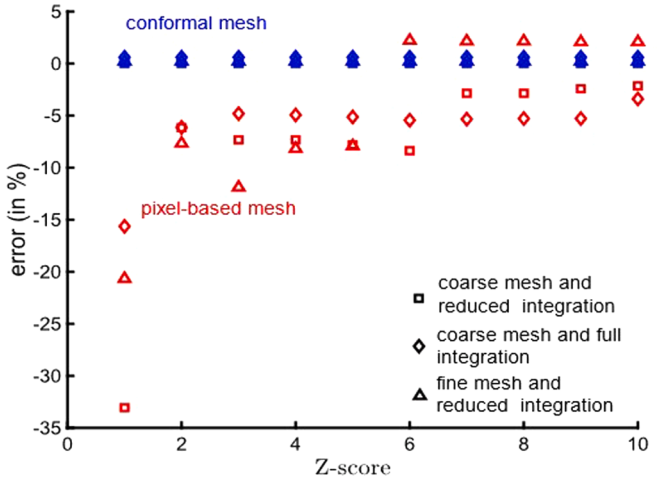

Fig. 8. The error in conformal and pixel-based meshes in a finite width plate with a circular hole at different values of z-score.

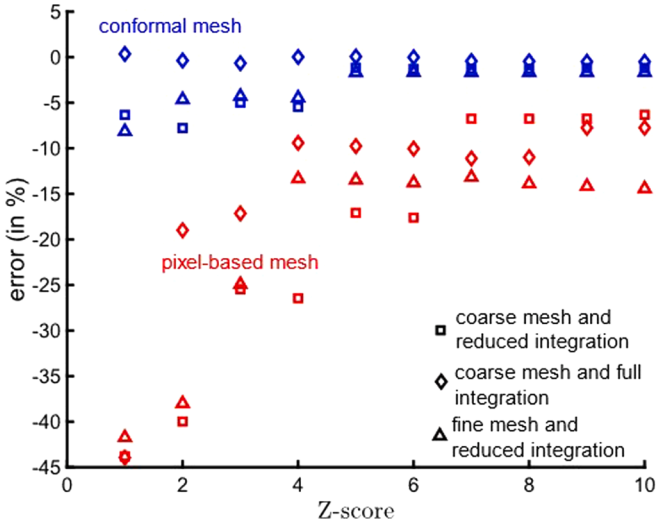

Fig. 9. The error in a conformal and pixel-based mesh in finite width plate with an elliptical hole at different values of z-score.

artificial stress concentration arising from the discretization method.

The maximum von Mises stress value at the zigzag boundary depends on the computational conditions such as type of elements, material systems, and mesh size. The performance of the extrapolation method was assessed in various cases for two-dimensional problems. The results are shown in Tables 3-6. From these tables, it is conclusive that the extrapolation method consistently gives a better estimate than the maximum von Mises stress predicted by pixelized mesh. Thus, the extrapolation method does account for the influence of computational conditions. However, the considered computational conditions are not exhaustive, as finite element studies have many element types. The analysis was restricted to the ones that we are most likely to use in our ongoing research of textile composites.

Furthermore, the degree of stress concentration depends on the type of stress. For the same loading conditions, the exaggeration of individual stress components is not uniform. As we were interested in the strength of the composite, we dealt with equivalent stress measures rather than individual stress components. The robustness of the proposed extrapolation method was verified by implementing it on the conformal mesh that does not exhibit artificial stress concentration. It was observed that the maximum von Mises stress predicted by the extrapolation method on the conformal mesh is within 1.5% of the realistic stress concentration. Thus, we believe that the extrapolation method is likely to be more helpful than harmful in the prediction of individual stress components or principal stresses.

4. Conclusions

In this study, we observed stress values of pixelized mesh, in general, are exaggerated due to artificial stress concentration. This effect was particularly severe in meshes with a full integration scheme followed by

Table 6
The comparison of maximum von Mises developed in a plate with an elliptical hole in the pixel-based mesh and conformal mesh. The values in parenthesis are the deviations calculated relative to maximum von Mises stress from conformal mesh.

mesh	Conformal mesh (MPa)	Extrapolation method on conformal mesh (MPa)	Pixel-based mesh (MPa)	Extrapolation method on pixel-based mesh (MPa)	Averaging scheme of Fang et al. on pixel-based mesh (MPa)
Coarse mesh and reduced integration	380	375 (-1.29%)	396 (4%)	354 (-7%)	303 (-20%)
Coarse mesh and full integration	378	378 (0.07%)	485 (28%)	338 (-11%)	303 (-20%)
Finer mesh and reduced integration	376	374 (-0.63%)	410 (9%)	327 (-13%)	338 (-10%)

a mesh of lower mesh size. Consequently, the maximum von Mises stress predicted by a pixelized mesh is inaccurate. We discussed an extrapolation method that can screen out the spurious/factitious stress concentration in pixelized meshes while preserving the physically meaningful stress concentration. This was achieved by using a data-driven method to identify a trustworthy region based on the z-score. This was helpful in separating the reliable stress data from the stresses that were affected by the artifact of zigzag mesh. It is true that the extrapolation method cannot be generalized to an arbitrary problem. However, the proposed extrapolation method can estimate the physically meaningful maximum stress to within 40% accuracy compared to the conformal mesh including adverse scenarios. Even though the example problems are limited to pixel-based 2-D meshes, the procedure can be applied to 3-D voxel meshes by following a similar approach.

CRediT authorship contribution statement

Hemanth Thandaga Nagaraju: Methodology, Formal analysis, Data curation, Investigation, Writing – original draft. **Bhavani V. Sankar:** Conceptualization, Methodology, Supervision, Writing – review & editing. **Nam-Ho Kim:** Conceptualization, Methodology, Supervision, Writing – review & editing. **Ghatu Subhash:** Conceptualization, Methodology, Funding acquisition, Supervision, Writing – review & editing.

Declaration of Competing Interest

The authors declare that they have no known competing financial interests or personal relationships that could have appeared to influence the work reported in this paper.

Acknowledgments

This research was performed under the Department of Energy (DOE) Nuclear Energy University Programs (NEUP) grant no. DE-NE0008773 to the University of Florida. The opinions expressed in this article are solely those of the authors and do not reflect those of the funding agency.

Data availability

The raw/processed data required to reproduce these findings cannot be shared at this time due to technical or time limitations.

References

[1] Tan P, Tong L, Steven GP. Modelling for predicting the mechanical properties of textile composites - A review. Compos Part A Appl Sci Manuf 1997;28:903–22. https://doi.org/10.1016/S1359-835X(97)00069-9.
[2] Gao X, Luo P, Yu G, Fang G, Song Y. Micro-XCT-based finite element method for prediction of elastic modulus of plane woven carbon fiber-reinforced ceramic matrix composites. J Compos Mater 2015;49:3373–85. https://doi.org/10.1177/0021998314562631.
[3] De Carvalho NV, Pinho ST, Robinson P. Reducing the domain in the mechanical analysis of periodic structures, with application to woven composites. Compos Sci Technol 2011;71:969–79. https://doi.org/10.1016/j.compscitech.2011.03.001.
[4] Marrey RV, Sankar BV. Micromechanical models for textile structural composites 1995.
[5] Sankar BV, Marrey RV. A unit-cell model of textile composite beams for predicting stiffness properties. Compos Sci Technol 1993;49:61–9. https://doi.org/10.1016/0266-3538(93)90022-9.
[6] Marrey RV, Sankar BV. A Micromechanical Model for Textile Composite Plates. J Compos Mater 1997;31. https://doi.org/10.1177/002199839703101202.
[7] Whitcomb JD, Chapman CD, Tang X. Derivation of boundary conditions for micromechanics analyses of plain and satin weave composites. J Compos Mater 2000;34:724–47. https://doi.org/10.1177/002199830003400901.
[8] Kier ZT, Salvi A, Theis G, Waas AM, Shahwan K. Estimating mechanical properties of 2D triaxially braided textile composites based on microstructure properties. Compos Part B Eng 2015;68:288–99. https://doi.org/10.1016/J.COMPOSITESB.2014.08.039.
[9] Akpoyomare AI, Okereke MI, Bingley MS. Enforcing periodic boundary conditions on general finite element discretisations of heterogeneous materials. High Perform Optim Des Struct Mater II 2016;1:129–42. https://doi.org/10.2495/hpsm160121. WIT Press.
[10] Kim HJ, Swan CC. Voxel-based meshing and unit-cell analysis of textile composites. Int J Numer Methods Eng 2003;56:977–1006. https://doi.org/10.1002/nme.594.
[11] Lin H, Brown LP, Long AC. Modelling and simulating textile structures using TexGen. Adv Mater Res 2011;331:44–7. https://doi.org/10.4028/www.scientific.net/AMR.331.44. Trans Tech Publications Ltd.
[12] Long AC, Brown LP. Modelling the geometry of textile reinforcements for composites: TexGen. Compos Reinf Optim Perform, Elsevier Ltd 2011:239–64. https://doi.org/10.1533/9780857093714.2.239.
[13] Fang G, El Said B, Ivanov D, Hallett SR. Smoothing artificial stress concentrations in voxel-based models of textile composites. Compos Part A Appl Sci Manuf 2016;80:270–84. https://doi.org/10.1016/J.COMPOSITESA.2015.10.025.
[14] Charras GT, Guldberg RE. Improving the local solution accuracy of large-scale digital image-based finite element analyses. J Biomech 2000;33:255–9. https://doi.org/10.1016/S0021-9290(99)00141-4.
[15] Hollister SJ, Riemer BA. Digital-image-based finite element analysis for bone microstructure using conjugate gradient and Gaussian filter techniques. In: Wilson JN, Wilson DC, editors. Proc. Vol. 2035, Math. Methods Med. Imaging II; 1993, p. 95–106. 10.1117/12.146616.
[16] Drach A, Drach B, Tsukrov I. Processing of fiber architecture data for finite element modeling of 3D woven composites. Adv Eng Softw 2014;72:18–27. https://doi.org/10.1016/J.ADVENGSOFT.2013.06.006.
[17] Smitheman SA, Jones IA, Long AC, Ruijter W. A voxel-based homogenization technique for the unit cell thermomechanical analysis of woven composites. ICCM Int Conf Compos Mater 2009.
[18] Thandaga Nagaraju H, Sankar BV, Subhash G, Kim NH, Haftka RT. Effect of curvature on extensional stiffness matrix of 2-D braided composite tubes. Compos Part A Appl Sci Manuf 2021;147:106422. https://doi.org/10.1016/j.compositesa.2021.106422.
[19] Karkkainen RL, Sankar BV. A direct micromechanics method for analysis of failure initiation of plain weave textile composites. Compos Sci Technol 2006;66:137–50. https://doi.org/10.1016/j.compscitech.2005.05.018.
[20] Fang G, Chen C, Meng S, Liang J. Mechanical analysis of three-dimensional braided composites by using realistic voxel-based model with local mesh refinement. J Compos Mater 2019;53:475–87. https://doi.org/10.1177/0021998318786541.
[21] Camacho DLA, Hopper RH, Lin GM, Myers BS. An improved method for finite element mesh generation of geometrically complex structures with application to the skullbase. J Biomech 1997;30:1067–70. https://doi.org/10.1016/S0021-9290(97)00073-0.
[22] Numerical gradient - MATLAB gradient n.d. https://www.mathworks.com/help/matlab/ref/gradient.html (accessed September 23, 2021).
[23] Savitzky A, Golay MJE. Smoothing and Differentiation of Data by Simplified Least Squares Procedures. Anal Chem 2002;36:1627–39. https://doi.org/10.1021/AC60214A047.
[24] Doitrand A, Fagiano C, Irisarri FX, Hirsekorn M. Comparison between voxel and consistent meso-scale models of woven composites. Compos Part A Appl Sci Manuf 2015;73:143–54. https://doi.org/10.1016/j.compositesa.2015.02.022.
[25] Pilkey WD, Pilky DF. Peterson's stress concentration factors. 3rd ed. Hoboken, N.J. : John Wiley; 2008.